LOW VELOCITY IMPACT RESPONSE OF THIN WALLED GRAPHITE/EPOXY CYLINDERS

Uday K.Vaidya[1], Chad Ulven[1], Terry Vandiver[2], and Robert Evans[2]

[1]North Dakota State University, Composites Research Laboratory
Department of Mechanical Engineering, Fargo, North Dakota, 58105 USA

[2]U.S.Army, Aviation and Missile Command (MICOM), Redstone Arsenal, Alabama, 35898 USA

SUMMARY : Helical and hoop wound graphite/epoxy (Gr/Ep) composite cylinders have been tested under low velocity impact (LVI) loading. The studies were conducted in two phases. In Phase I, the impact energy levels ranged from 1 to 6 ft-lbs, while in Phase II, the impact energy levels ranged from 35 ft lbs-50 ft lbs. Nondestructive evaluation (NDE) tests (ultrasonic and vibration) were conducted to assess the damage evolution in the cylinders. Ultrasonic NDE was utilized to assess process integrity and to map the impact damage. Vibration based NDE tests were conducted prior to, and after impact to determine modal response (frequency and damping ratio) of the composite cylinders under a simply supported boundary condition. The microstructure of some of the cylinders has also been studied by sectioning them at impact locations.

KEYWORDS: Graphite/Epoxy (Gr/Ep), Composite cylinder, Low Velocity Impact (LVI), Nondestructive Evaluation (NDE)

INTRODUCTION

During the last two decades, the use of advanced composites, especially continuous fiber-reinforced polymer composites in high performance structural applications has increased considerably. For the most part, this increased use of composites has been driven by the desire to reduce structural weight, and thereby improve performance. Polymer matrix composites offer much higher specific strength and specific stiffness than those offered by aluminum and steel. While the initial cost of a composite structure is typically higher than that of a metallic counterpart, for those applications that benefit greatly from weight reduction during the service life, composites are cost-effective candidate materials. Not surprisingly, many of the areas in which composites have been applied are associated with high-performance transportation systems, such as aircraft, spacecraft, high-speed rail, and racing automobiles.

One area in which composites have been used rather extensively is for fabricating rocket motor cases [1]. These structures can be readily manufactured by filament winding, which is, as far as composite fabrication techniques are concerned, a relatively inexpensive method for producing composite structures. The reduction in structural weight afforded by fiber-reinforced composites translates into significant increases in rocket performance.

In terms of failure, composites exhibit brittle behavior. Complex damage stages, which include matrix cracking, delamination, and fiber fracture, can develop in these material systems, early in the load history, and often there is little or no surface indication that such micro structural damage is present. This is of particular concern when the composite is subjected to unanticipated load excursion. For example, when a composite structure is subjected to LVI, micro structural damage can be introduced [2-3]. For LVI, there may be little or no indentation of the surface to indicate that the impact occurred or the severity of the resulting damage state.

Figure 1. Hoop and helical wound Gr/Ep cylinders

The current study deals with investigating and understanding the LVI response of Gr/Ep cylinders. A set of hoop wound, and helical wound cylinders were investigated for LVI and NDE characteristics.

EXPERIMENTAL

Ultrasonic C-Scan Testing: A total of twelve (six hoop wound) and (six helical wound) Gr/Ep cylinders (Fig.1) were studied. The cylinders had an average weight of 274 gms (0.604 lbs), length 319 mm (12.5"), wall thickness 1.5 mm (0.06"), inner diameter 127.5 mm (5.01") and outer diameter 129 mm (5.07"). The lay-up comprised three layers. All cylinders were subjected to pre-and post-impact ultrasonic C-scan testing. A Testtech system with a five-axis robot in conjunction with a USP-12 Krautkramer Branson ultrasonic pulser receiver was used for ultrasonic testing of the cylinders. The following approach was taken in scanning the cylinders. The cylinder was held in a grooved head, which was attached to a rack and pinion arrangement. It was ensured that the central rod of the fixture was parallel to the axis of the cylinder. A 5 MHz pulse-echo immersion type ultrasonic transducer was focused with respect to the uppermost position on the cylinder. A developed view of the cylinder was obtained by indexing the cylinder on the rack and pinion fixture.

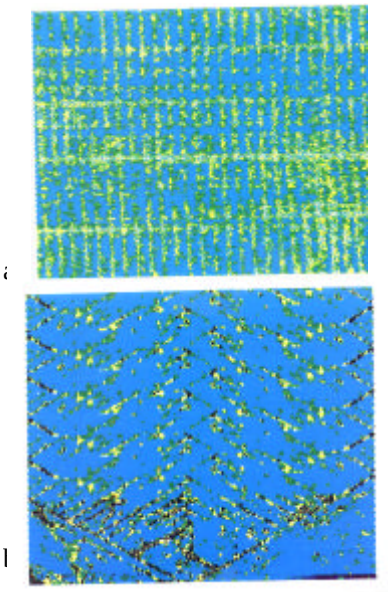

Figure 2. Ultrasonic C-scan of a) hoop and b) helical wound Gr/Ep cylinder

Figures 2a and 2b represent typical ultrasonic C-scans obtained from the hoop and helical wound cylinders respectively. The fiber bundles in the hoop and helical directions are clearly resolved. It is further seen that several crossover points related to the filament winding process on the inside ply of the cylinders were mapped accurately as well.

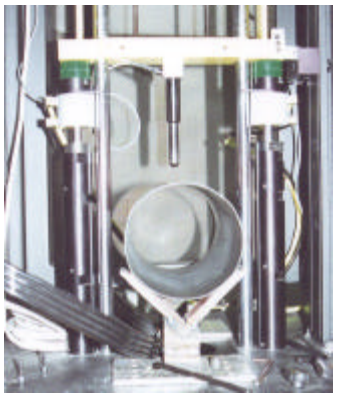

Figure 3. LVI testing of Gr/Ep cylinder

LOW VELOCITY IMPACT TESTING

An 8210 Dynatup drop weight impact testing equipment was used for the LVI testing. Two V-shaped angles, with thin rubber pads at the support bonded to the resting edge of the cylinder were bolted to the 8210-specimen chamber (Fig.3). The cylinder rested on the fixture in a simply supported boundary condition. A pneumatic assist rebound arrestor mechanism was utilized such that the cylinder would be subjected to a single impact event. The force-time and load-energy curves were recorded for all impact levels. The cylinders were impacted with normal incidence to the longitudinal axis. In phase one, each hoop and helical wound cylinder was impacted at 1, 2, 3, 4, 5 and 6 ft.lb respectively. Post-impact ultrasonic and vibration evaluation was conducted. Noting that these levels did not cause discernable damage (either by visual inspection or ultrasonic C-scan), the impact tests were repeated on the cylinders in phase two. The 1 ft-lbs and 6 ft-lbs impacted cylinders were not tested for phase two tests. The 2, 3, 4 and 5 ft.lb-impacted cylinders were impacted on their diametrical opposite end (with reference to the location from phase one impact) at the following energy levels. The cylinder impacted in phase one 5 ft-lbs was subjected to 50 ft-lbs in phase two, the 4 ft-lbs of phase one to 45 ft-lbs in phase two, the 3 ft-lb of phase one to 40 ft-lb in phase two and the 2 ft-lbs of phase one to 35 ft-lbs in phase two. The logical reasoning behind this was to have a descending damage state in the cylinders.

Phase One Tests: The force-time histories from phase one impact are shown in Figs. 4 and 5 for the hoop and helical wound cylinders respectively. Multiple load-drops are observed in the cylinder force-time histories. When the striker makes contact with the cylinder, the cylinder goes into flexure. Over 14 msec of contact, the striker makes and breaks contact at least three to four times. The convex contour of the surface appears to exaggerate this phenomenon in the force-time histories. This behavior is seen consistently for all the cylinders tested. The peak load for the 6 ft-lbs impact under phase one was 113 lbs from the hoop wound cylinders and 68 lbs from the helical wound cylinders. As expected the magnitude of the peak load increases with impact energy levels.

The following observations can be made for the two cylinder types. The hoop wound cylinders typically show higher peak loads and higher stiffness than the corresponding helical wound cylinders tested at the same energy levels. The slope of the force-time curve is higher for the hoop wound cylinders than the helical wound ones. With increase in impact energy, the peak loads and energy absorbed are seen to increase in accordance. For impact energies 1-6 ft-lbs, the damage is not significant. Figure 6 compares the typical force-time-energy history for a hoop Vs helical wound cylinder impacted with 6 ft-lb energy.

Phase Two Tests: In phase two (35, 40, 45 and 50 ft-lb) impacts, the force-time-energy histories for the hoop and helical wound cylinder are compared. A comparison of the force-time-energy histories for the 50 ft-lb energy impact is shown in Fig. 7. The peak loads are much higher. Typically, the hoop wound cylinder exhibit a peak load of 197 lbs, while the helical wound cylinders exhibit a peak load of 154 lbs. The force-time curves here show visible indications of deviation from their trend. In the trailing part of the first load peak, multiple load oscillations (not corresponding to localized noise) are observed, which appear to correspond to damage initiation and development in the cylinders. From the C-scans this damage is deduced to occur due to fracturing of the inner helical ply in the hoop wound cylinders, and due to inner ply cracking in case of the helical wound cylinders. Furthermore, the hoop wound cylinders being stiffer, the damage area is larger.

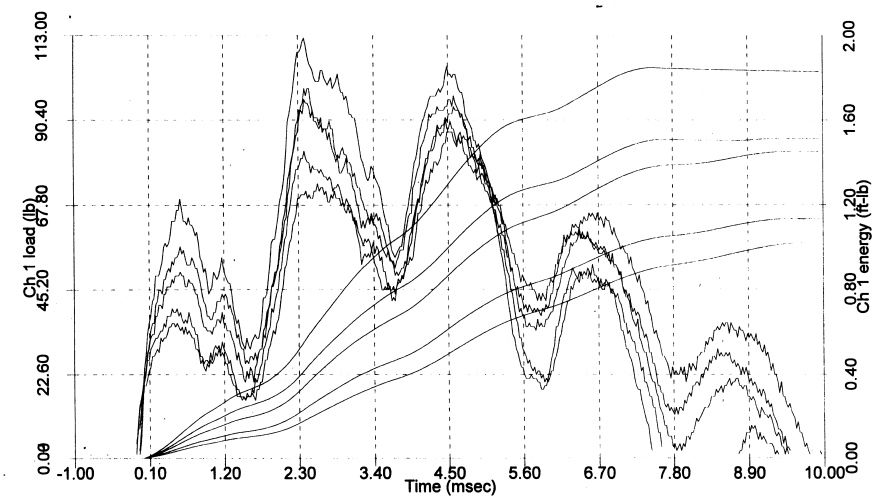

Figure 4. Force-time-energy history of hoop wound Gr/Ep cylinder (1-6 ft lb impact energy, shown in ascending order in the curves)

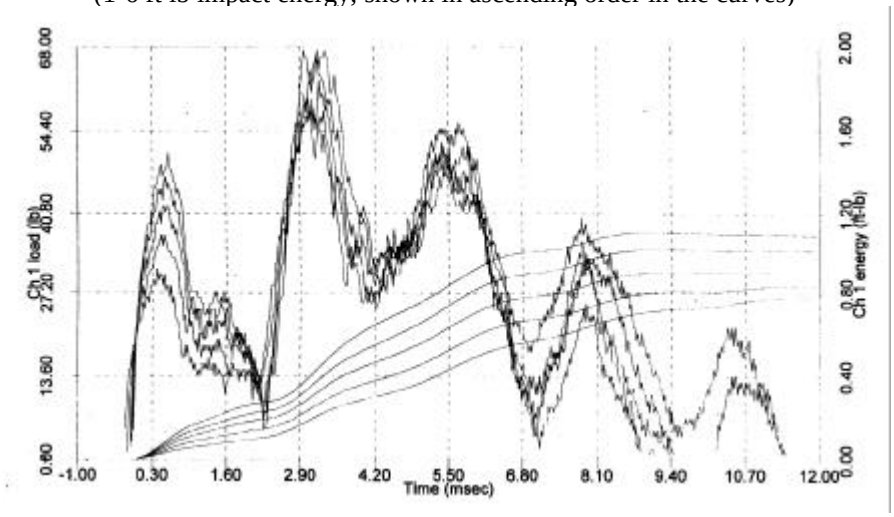

Figure 5. Force-time-energy history of helical wound Gr/Ep cylinder (1-6 ft lb impact energy, shown in ascending order in the curves)

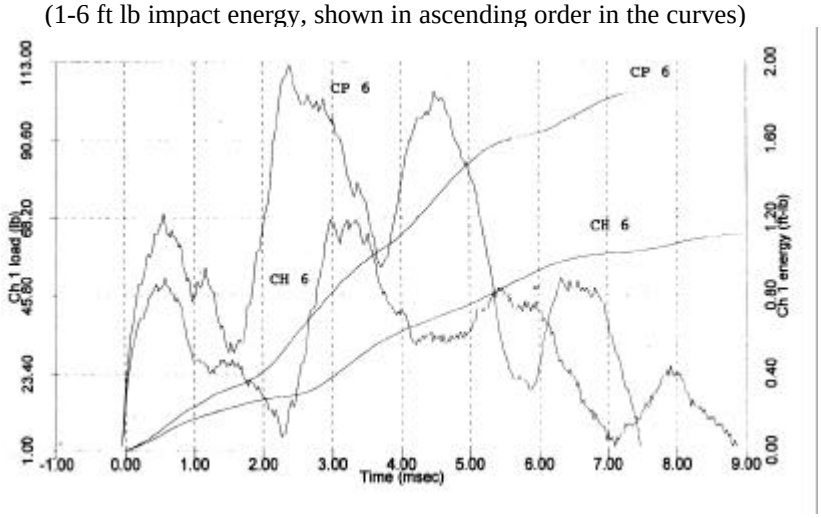

Figure 6. Force-time-energy history of hoop wound Vs. helical wound Gr/Ep cylinder (6 ft-lb impact energy) CP- hoop, CH- helical

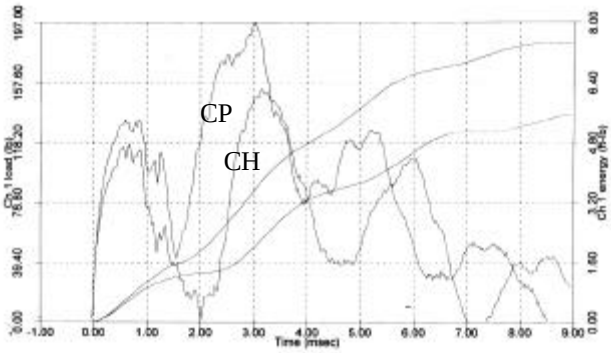

Figure 7. Force-time-energy history of hoop Vs. helical wound Gr/Ep cylinder (50 ft lb impact energy) CH-helical, CP-hoop

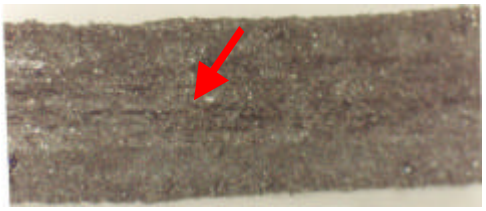

Figure 8. Damage mode in hoop wound cylinder under LVI - 50 ft-lb impact. *Arrow indicates debond location.*

Micro structural Studies: Adjacent to the point of impact, ring specimens were sectioned. The specimens were then subjected to microscopic inspection along the thickness and for surface observations, to observe fiber fracture and interply failure. Figure 8 represents a typical failure mode. The initiation of damage is through interply debond cracks. These cracks then coalesce to form long scale delaminations. There is little evidence of fiber fracture. The primary mode of damage is debonding between the first and second layer at lower impact energies, and between second and third layer as well at higher impact energies. For the helical wound samples, the tension side (underside) of the specimens exhibited tendency for tows to separate, but not fracture.

VIBRATION BASED NONDESTRUCTIVE EVALUATION

The vibration response of the cylinders was measured using a dual channel Bruel and Kjaer (B&K) 2032 frequency analyzer. A B&K 8001 impedance head was attached to a B&K 4810 mini-shaker via a 5" flexible stringer. The mini-shaker with the impedance and stringer was mounted in an inverted manner on a steel table (Fig. 9). The height of the steel table was adjusted such that the cylinder with V-blocks could be set up under the table in the same simply supported manner that was used to impact them. The position was so adjusted that the impedance head made exact contact with the maximum position of the cylinder. A small amount of bees wax was placed between the impedance head and the cylinder to assure proper vibration contact. The impedance head in all cylinders tested made contact 2" away from the impact location of the cylinders. The shaker was excited using random noise excitation. The frequency response function and damping ratio value was obtained using a half power interval (3 dB bandwidth) method reported elsewhere [4]. The damping ratio (ζ) is given by :

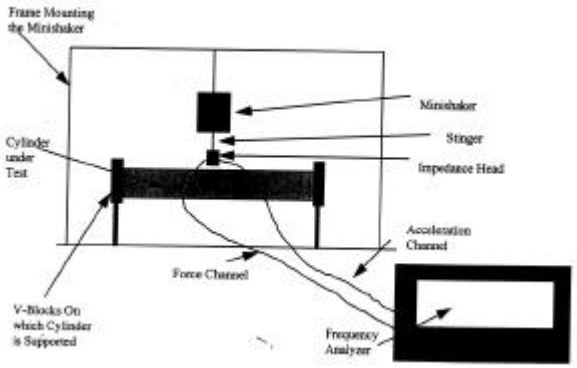

Figure 9. Vibration testing of Gr/Ep cylinder

$$\zeta = f_2 - f_1/2f_n$$

where f_1 and f_2 are the upper and lower bounds of the 3dB reduction around the resonance frequency, and f_n is the peak value (at resonance).

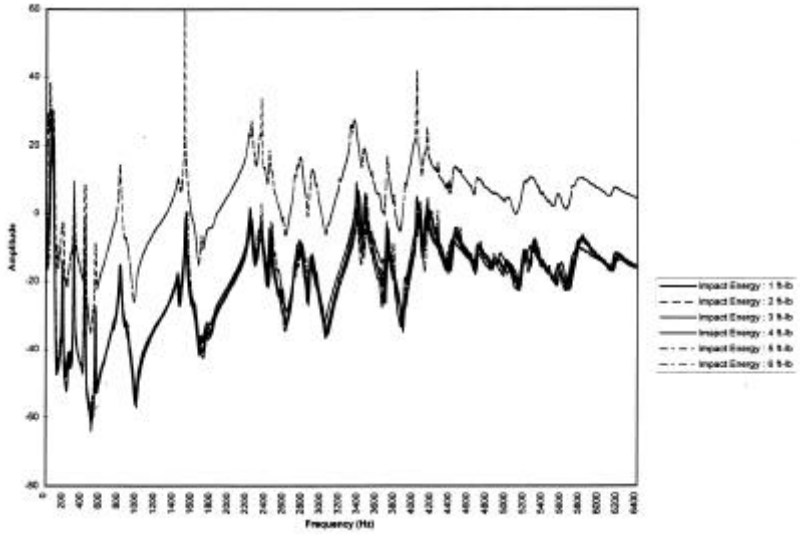

Figure 10. FRF of hoop wound cylinders after 1-to 6 ft.lb impact

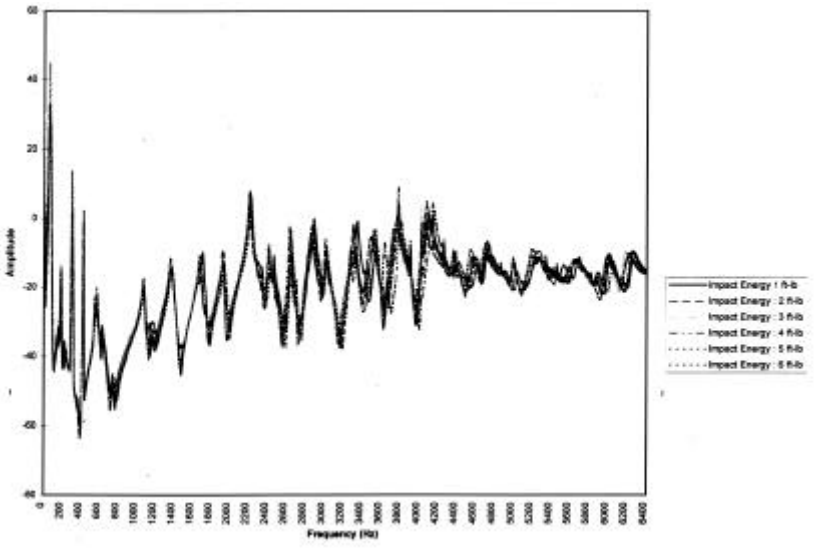

Figure 11. FRF of helical wound cylinders after 1-to 6 ft.lb impact

Figure 10 represents a typical frequency response function (FRF) obtained from a hoop wound cylinder, in comparison to a helical wound cylinder (Fig. 11). The modal density of the helical wound cylinder is higher (~20 modes over a frequency range of 0-6400 Hz as opposed to ~12 modes over the same frequency range). The fundamental frequency of the hoop wound is 304 Hz as compared to the helical wound which is 176 Hz, indicating that the hoop wound cylinders are much stiffer than the helical wound cylinders. Typically the first mode is 42% lower in the helical wound cylinder as compared to hoop wound. The subsequent modes are 20-25% lower in magnitude as compared to the helical wound cylinders. The impact events 1 ft-lb to 6 ft-lb did not show any notable changes in the frequency. However, the higher energy (phase two) impacts (35 ft-lb to 50 ft-lb) show that several peaks in the FRF are much damped as compared to their corresponding phase one measurements, as can be seen from Figs. 12 and 13.

The damping ratio of the cylinders was found to be highly sensitive to micro structural damage state. The damping ratio of the helical wound cylinders is higher (as compared to the hoop wound cylinders) at all impact levels that the specimens were subjected to (Table 1). The typical average damping ratio measured from the hoop wound cylinders is 0.008 for mode 1 while for the helical wound cylinders, it was 0.011 (~38% higher than the hoop wound). The damping ratios measured

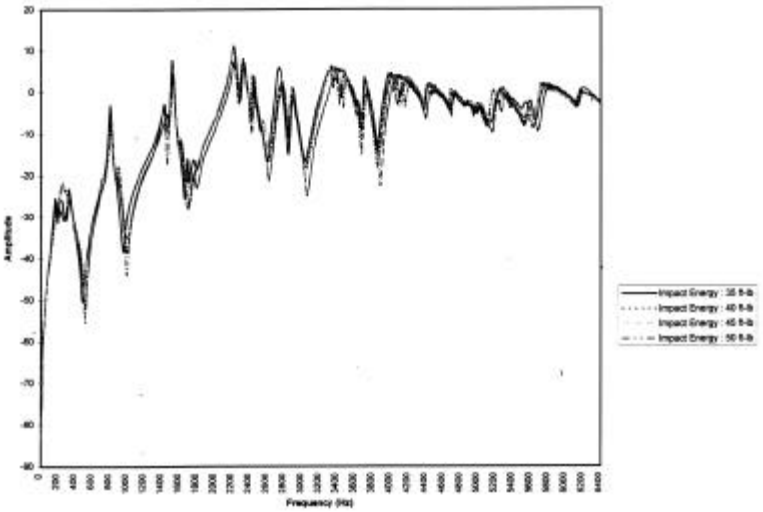

Figure 12. FRF of hoop wound cylinders after 35-to 50 ft.lb impact

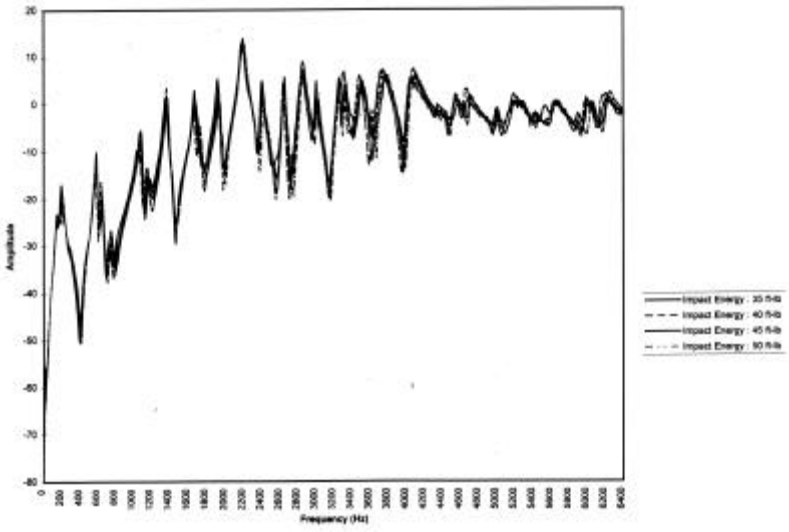

Figure 13. FRF of helical wound cylinders after 35-to 50 ft.lb impact

for cylinders impacted from 1 to 6 ft-lb were found to be in the above range. The damping ratios increased dramatically when the cylinders were subjected to 35-to 50 ft-lb impact. For these impact energies also the helical wound cylinders exhibited higher damping as compared to the hoop wound. The damping ratio range for the helical wound cylinders averaged at 0.076, while for the hoop wound the average value was 0.032 (137.5% higher for helical wound as compared to hoop). The presence of angle plies in the helical winding, that provide high shear damping (frictional effects) when the cylinder is subjected to flexural vibration. This also confirms that micro structural damage condition exists in the cylinders (more sensitivity to damping ratio changes than natural frequency).

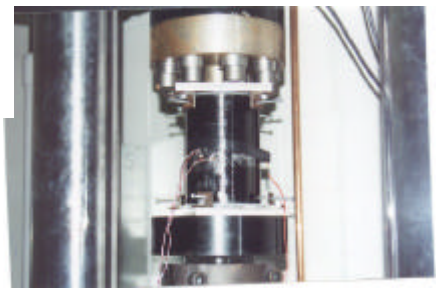

Figure 14. CAI and AE testing of Gr/Ep cylinder

Post-Impact Compression-After-Impact (CAI) Testing with Acoustic Emission (AE) Monitoring

Following LVI testing and post-impact ultrasonic and vibration based NDE, some of the cylinders were subjected to CAI tests (Fig. 14). The virgin and the 50 ft-lb impacted helical and hoop wound cylinders are considered in this paper. ASTM D5449 was adopted in the CAI testing [5]. According the ASTM standard, in order to prevent global buckling during axial loading, the cylinders had to possess a length to diameter ratio of 1.375. In order to satisfy this condition, the cylinders had to machined from either sides to parallel surfaces to a length of 7.5" (maintaining the geometric center at the impact location) from their original length of 12.5". Strain gages in the axial and hoop directions were mounted on a helical

wound cylinder to verify that global buckling did not occur. The cylinders were potted at their ends in epoxy paste to prevent brooming along the edges. The cylinders were subjected to CAI in a fixture that constrains the cylinder between four diagonal screws on the either end. An acoustic emission (AE) sensor (150 kHz) resonant frequency, with a 100-300 kHz filter was strapped to the geometric center of the cylinders using a stretchable black electrical tape. The amplitude threshold of the AE events was set at 45 dB. The data obtained from the AE sensor was plotted as three-dimensional histograms representations of AE energy (ENG), duration (DUR), and amplitude (AMP) with respect to test time (seconds).

Table 1. Damping Ratio Measured from Gr/Ep Cylinders

Impact Energy (ft-lb)	Hoop Wound		Helical Wound	
	Damping Ratio (ζ)			
	Mode 1	Mode 2	Mode 2	Mode 2
1	0.0090	0.0050	0.0110	0.0110
2	0.0087	0.0060	0.0095	0.0220
3	0.010	0.0030	0.0150	0.0080
4	0.0085	0.0025	0.0090	0.0065
5	0.0085	0.0028	0.0160	0.0120
6	0.0092	0.0025	0.0090	0.0110
35	0.0390	-	0.0750	-
40	0.0250	-	0.0900	-
45	0.0350	-	0.0690	-
50	0.0280	-	0.0700	-

- did not measure Mode 2 damping ratio for 35-50 ft-lb impacted samples

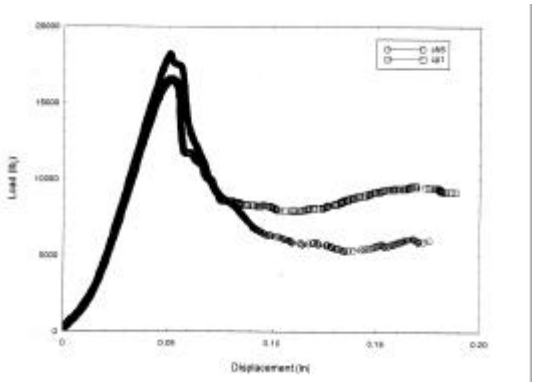

Figure 15. CAI test of Gr/Ep cylinder. Cp-hoop, Ch-helical

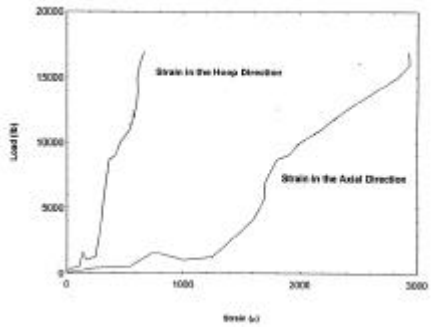

Figure 16. Strain gage readings along hoop and axial direction for a *helical* wound cylinder under CAI loading

Figure 15 represents the typical load-displacement curve obtained through CAI failure of a hoop and helical wound cylinder. The CAI compression load, of the hoop wound cylinders subjected to 1 ft-lb impact was 16565 lbs, for 50 ft-lb impact it was 16517 lbs. For the helical wound, the specimen subjected to 1 ft-lb was 18417 lbs, for 50 ft-lb it was 18224 lbs. The failure load followed the impact event the specimens were subjected to. The primary mode of failure was by localized buckling of the cylinders followed by fiber fracture in the hoop wound cylinders, and shear ply cracking in case of the helical wound cylinders. For the helical wound cylinders, the failure originates along the helical winding, and there is a tendency of the inner side windings to separate (debond) from each other. The matrix cracking during lateral movement of these plies are

clearly captured as acoustic events by the AE sensor. Adjacent shear cracks travel parallel to each other till they meet the cross-over point in the inside of the cylinder, and the debond deflects and assumes the direction of the cross-over windings. This was noticed in all the helical wound plies. Both hoop and helical wound cylinders, did not exhibit catastrophic failure. The load-displacement curve (Fig. 15) showed a typical non-linear portion. The compression failure load of the helical wound cylinder is higher by about 10% as compared to the hoop wound cylinder. The strain-to-buckling load failure is almost similar for both the specimen types. Strain gages were mounted for a helical wound cylinder with strain gages mounted to measure axial and hoop strain developed during CAI loading. The strain gage data (Fig. 16) shows that deformation of the helical plies is much more pronounced in the axial direction as compared to the hoop direction.

Acoustic Emission Testing: Figure 17a represents time vs. amplitude (AMP) vs. energy (ENG) in a three-dimensional (3D) histogram distribution plot for the hoop wound cylinder under CAI loading. The AMP is represented in decibels (dB), Energy (ENG) is unit less, and time is represented in seconds. Typically, matrix micro cracking is represented by low energy <45 and low amplitude (45-55 dB) events are seen from the start of loading until 30 sec of loading. Beyond this, the phenomenon of fiber bundle fracture in the hoop rings is represented by the energy increases significantly to values exceeding 100 with corresponding activity in the 55-to 100 dB ranges. In addition, matrix cracking continues till failure. At the onset of final failure, the energy and amplitude of the events increase dramatically.

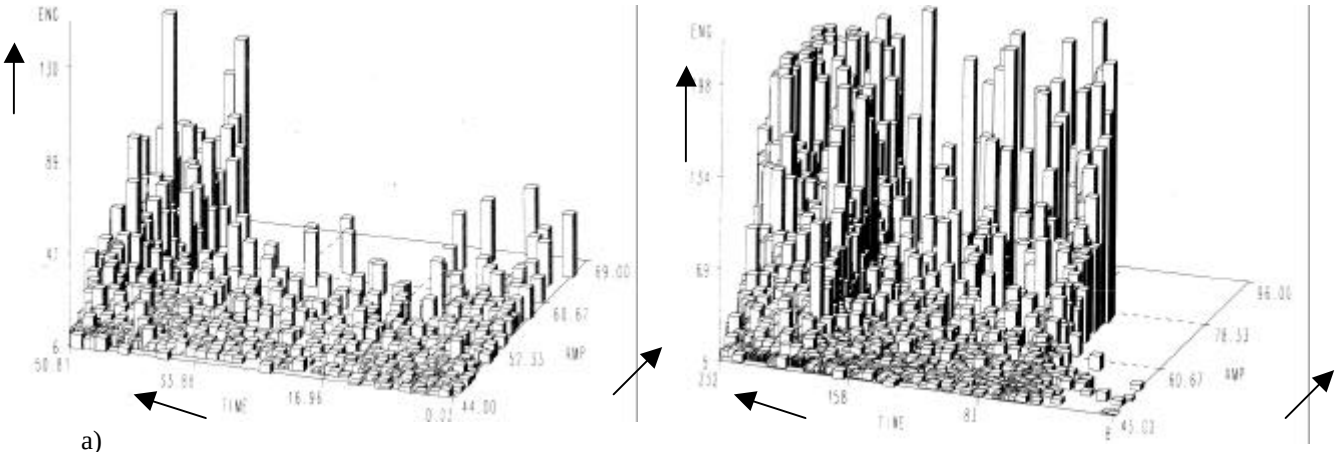

a) b)

Figure 17. Acoustic emissions from CAI tests on Gr/Ep cylinder a)hoop wound, and b) helical wound). *Note : The x-axis is read from the right end of the TIME scale towards the left.*

Figure 17b represents similar 3D-histogram plot for a helically wound cylinder under CAI loading. Unlike the hoop wound cylinders, the helical wound cylinder failed by plies shearing in the direction of winding of the plies. The inner side of the cylinders as indicated earlier exhibited fiber bundle separation parallel to each other until the crossover points. This separation or matrix macro cracking (debonding along the plies) are frictional events (high energy features), and are seen to originate at about 30 sec into the loading cycle. The high energy (>100) and high amplitude (80-100 dB) events continue to dominate till failure, in addition to matrix micro cracking events, which occur until failure also. The number of AE events increased dramatically as failure approached in the helically wound cylinder as well.

CONCLUSIONS

- The low velocity drop weight impact experiments on simply supported hoop and helical wound cylinders indicated that no notable damage was evident in the case of impact energy levels of 1 ft-lb to 6 ft-lb. This was validated through both ultrasonic and vibration NDE.
- The threshold impact energy level to cause significant damage in the Gr/Ep cylinders was determined to be 35 ft-lb. The impact response of the cylinders shows the presence of micro structural damage in the trailing portion of the force-time curve. Micro structural observations show interply debonding and delamination initiation between the first and second and in some cases second and third layers.
- Vibration based NDE was highly effective in determining that damping ratio dramatically increased in the 35-50 ft-lb impacted cylinders due to creation of the damage. The damage was not detected by resonance frequency changes. The helical wound cylinders exhibit 25-42% higher damping ratios at all flexural modes in comparison to the hoop wound cylinders. This is attributed to shear damping of the helical plies.
- The primary defect detectable by ultrasonic C-scan was debonding on the innermost lining in the helical wound cylinders, and some fiber/matrix debonding in the hoop wound cylinders.
- Compression after impact response of the cylinders follow their impact event history; typically the helical wound cylinders show higher CAI values than their corresponding hoop wound cylinders, due to lower damage state in the helical wound cylinder.
- Acoustic emission was effective in determining matrix cracking when the tows of the helical winding tended to separated during axial compression and warning of imminent failure; and as fiber bundle fracture along the hoop winding occurred in the case of the hoop wound cylinder.

REFERENCES

1. Highsmith, A.L, Ledbetter, F.E, Nettles, A, and Russel. S.S., "Low Velocity Impact Damage in Filament-Wound Composite Pressure Bottles", *Journal of Composites Technology and Research (JCTRER)*, 1996. Vol.18, No.2, April, pp. 109-117.
2. Schmueser, D.W. and Wickliffe L.E., "Impact Energy Absorption of Continuous Fiber Composite Tubes", *Transcations of ASME, Journal of Engineering Materials and Technology*, 1987. Vol.109, January, pp. 72-77.
3. Lagace, P.A. and Wolf E., "Impact Damage Resistance of Several Laminated Materials Systems", *AIAA Journal*, 1995. Vol.33, No.6, June. pp. 1106-1113.
4. Vaidya U.K., "Nondestructive Evaluation of Graphite Fiber Based Composites using Acoustic and Vibration Techniques", 1993. Ph.D Dissertation, Auburn University, Alabama.
5. "Standard Test Method for Transverse Compressive Properties of Hoop Wound Polymer Matrix Composite Cylinders", 1993. *ASTM D5449/D5449M-93*, American Society for Testing Materials, Philadelphia, PA.

ACKNOWLEDGMENTS

Research support provided by U.S. Army MICOM, Redstone Arsenal under the grant number DAAH01-96-P-R015 is highly appreciated. Mr. Terry Vandiver of U.S.Army MICOM served as the technical monitor. Assistance from Mr.Terry Vandiver and Mr. Robert Evans from MICOM is gratefully acknowledged. Dr. Steve Gross, Auburn University, Alabama lent the ultrasonic test fixture. The authors express their sincere thanks for his help. The encouragement provided by Dr. Shaik Jeelani, Tuskegee University - Center for Advanced Materials is also hereby acknowledged.